View metadata, citation and similar papers at core.ac.uk

brought to you by CORE

provided by Elsevier - Publisher Connector

Neoplasia • Vol. 9, No. 6, June 2007, pp. 479–486

www.neoplasia.com

Hyaluronic Acid–Paclitaxel: Antitumor Efficacy against CD44(+) Human Ovarian Carcinoma Xenografts[1]

Edmond Auzenne, Sukhen C. Ghosh, Mojgan Khodadadian, Belinda Rivera, David Farquhar, Roger E. Price, Murali Ravoori, Vikas Kundra, Ralph S. Freedman and Jim Klostergaard

The University of Texas M. D. Anderson Cancer Center, Houston, TX 77339, USA

Abstract

Numerous human tumor types, including ovarian cancer, display a significant expression of the CD44 family of cell surface proteoglycans. To develop tumor-targeted drugs, we have initially evaluated whether the CD44 ligand hyaluronic acid (HA) could serve as a backbone for paclitaxel (TXL) prodrugs. HA-TXL was prepared by modification of previous techniques. The *in vitro* cytotoxicity of HA-TXL against the CD44(+) human ovarian carcinoma cell lines SKOV-3ip and NMP-1 could be significantly blocked by preincubation with a molar excess of free HA. Female nude mice bearing intraperitoneal implants of NMP-1 cells were treated intraperitoneally with a single sub–maximum tolerated dose dose of HA-TXL or with multiple-dose regimens of paclitaxel (Taxol; Mead Johnson, Princeton, NJ) to determine the effects of these regimens on host survival and intraperitoneal tumor burden, with the latter being assessed by magnetic resonance imaging. NMP-1 xenografts were highly resistant to Taxol regimens, as host survival was only nominally improved compared to controls (T/C ~ 120), whereas single-dose HA-TXL treatment significantly improved survival in this model (T/C ~ 140; *P* = .004). In both NMP-1 and SKOV-3ip models, MR images of abdomens of HA-TXL–treated mice obtained shortly before controls required humane sacrifice revealed markedly reduced tumor burdens compared to control mice. This study is among the first to demonstrate that HA-based prodrugs administered locoregionally have antitumor activity *in vivo*.

Neoplasia (2007) **9,** 479–486

Keywords: Hyaluronic acid, CD44, paclitaxel, prodrug, human ovarian carcinoma.

Introduction

The majority of newly diagnosed ovarian cancers extend beyond the ovary and, in particular, involve the peritoneum [1–5]. Following surgical debulking, adjuvant chemotherapy treatment with platinum-containing and taxane-containing regimens results in high initial response rates, but most patients relapse with drug-resistant disease, hence the poor 5-year survival rates [1–6]. In a very noteworthy development, recent clinical trial results have provided compelling evidence that intraperitoneal administration of these drugs results in markedly improved survival in small-volume disease patients compared to intravenous administration [7–10]. This is an encouragement to develop new agents and/or drug formulations for intraperitoneal therapy.

Macromolecular drug copolymers [e.g., poly-L-glutamic acid–paclitaxel (PGA-TXL or XYOTAX)] have been developed as one approach to overcoming drug resistance. In preclinical and clinical studies, XYOTAX has demonstrated reduced toxicity, enhanced tumor accumulation, and greater antitumor efficacy compared to paclitaxel (Taxol; Mead Johnson, Princeton, NJ) [11–16]; of note, this paclitaxel prodrug is in advanced clinical trials in ovarian cancer, non–small cell lung cancer, and other carcinomas [17–22].

We reasoned that whereas PGA-TXL is likely restricted to uptake by fluid-phase pinocytosis, a paclitaxel copolymer that could exploit the selectivity and efficiency of receptor-mediated uptake might demonstrate even greater improvements in toxicity/efficacy parameters. The CD44 proteoglycan family, comprised of a parental form and 10 or more isoforms that are major receptors for hyaluronic acid (HA), is expressed in as high as ~ 90% of fresh samples from primary human ovarian tumors or peritoneal implants [23–29]. We proposed, as have others, that an HA backbone in a paclitaxel (TXL) copolymer (HA-TXL) might allow efficient and specific receptor-mediated prodrug uptake by CD44. The use of a hydrophilic HA backbone would both overcome the limited aqueous solubility of paclitaxel without resorting to the use of an excipient as in Taxol and would allow multiple sites for paclitaxel loading onto a single HA scaffold to be internalized by one or more CD44 molecules.

In the current study, we prepared a lead formulation of HA-TXL and evaluated its toxicity parameters, as well as its antitumor activity, in two CD44(+) human ovarian carcinoma nude mouse xenograft models. Our results, the first to establish these *in vivo* characteristics of such an HA-based prodrug,

Address all correspondence to: Jim Klostergaard, 1515 Holcombe Boulevard, Houston, TX 77030. E-mail: jkloster@mdanderson.org

[1]This study was supported by DOD Ovarian Cancer Research Program grant DAMD17-00-1-0726 (to J.K.) and by a grant (to R.E.P.) from the Ovarian Cancer SPORE awarded to the M. D. Anderson Cancer Center.

Received 2 March 2007; Revised 20 April 2007; Accepted 23 April 2007.

Copyright © 2007 Neoplasia Press, Inc. All rights reserved 1522-8002/07/$25.00

DOI 10.1593/neo.07229

indicate that even a single intraperitoneal administration of a sub-MTD dose of HA-TXL resulted in antitumor efficacy: reduced or eliminated tumor burden and prolonged survival compared to controls. We propose that further development of this targeted prodrug approach is warranted.

Materials and Methods

Cell Lines

A cisplatin (CDDP)–resistant cell line was first developed from parental OVCAR-3 cells (American Type Culture Collection, Manassas, VA) by *in vitro* incubation with increasing concentrations of CDDP [30]. Cells surviving several rounds of selection in CDDP-containing medium were cloned by limiting dilution, expanded, and retested for CDDP resistance. NMP-1 cells were derived from ascites of nude mice into which these CDDP-resistant OVCAR-3 cells had been implanted intraperitoneally [15,31].

The origin of the SKOV-3 ovarian adenocarcinoma cell line has been described previously [32,33]. The SKOV-3ip cell line used in the current study was derived from it by selection from an intraperitoneally implanted SKOV-3 xenograft, provided through the courtesy of Dr. I. J. Fidler.

HA-TXL Synthesis

HA ($\sim$ 40 kDa) was provided by K3 Corporation (Great Falls, VA). 1-Ethyl-3-[3′-(dimethylamino)propyl]carbodiimide (EDCI), diphenylphosphoryl chloride, adipic dihyrazide (ADH), succinic anhydride, *N*-hydroxysuccinimide (NHS), and triethylamine were purchased from Sigma-Aldrich Co. (Milwaukee, WI). Paclitaxel (Taxol) was purchased from HandeTech Development Co. (Houston, TX). All solvents were of reagent or high-performance liquid chromatography (HPLC) grade.

Analytic instrumentation Nuclear magnetic resonance (NMR) spectral data were obtained on a 300-MHz or a 500-MHz Bruker Advance Spectrometer (Fallanden, Switzerland). UV–Vis spectra were recorded on a Perkin-Elmer spectrometer (Perkin-Elmer, Waltham, MA). HPLC was carried out on a Waters Model 2695 system (Waters Corporation, Milford, MA) equipped with a C-18 column and a 2996 photodiode detector using H_2O–CH_3CN (60:40) as eluent at a flow rate of 1 ml/min.

Synthesis of Taxol–NHS ester The reported synthesis of Luo and Prestwich [34] and Luo et al. [35] was followed. To a stirred solution of paclitaxel (540 mg, 0.63 mmol) and succinic anhydride (76 mg, 0.76 mmol) in CH_2Cl_2 (25 ml) at room temperature was added dry pyridine (513 μl, 6.3 mmol). This reaction mixture was stirred for 3 days at room temperature and then concentrated *in vacuo*. The residue was dissolved in CH_2Cl_2 (5 ml), and the product was purified by silica gel column chromatography (ethyl acetate–hexane, 1:1) to yield Taxol-2′-hemisuccinate as a white solid (85%).

N-hydroxysuccinimido diphenyl phosphate (SDPP) was prepared from diphenylphosphoryl chloride, NHS, and triethylamine in CH_2Cl_2, as previously described [34,35]. The crude product was triturated with ether, dissolved in ethyl acetate, washed with H_2O, and dried over $MgSO_4$. The concentration of the organic layer *in vacuo* gave pure SDPP (85%).

To a solution of Taxol–hemisuccinate (300 mg, 0.31 mmol) and SDPP (164 mg, 0.46 mmol) in acetonitrile (15 ml) was added 175 μl (1.2 mmol) of triethylamine. The reaction was stirred for 6 hours at room temperature and then concentrated *in vacuo*. The residue was dissolved in ethyl acetate/hexane and purified by silica gel column chromatography (ethyl acetate–hexene, 1:2). Taxol–NHS ester was dried for 24 hours *in vacuo* at room temperature to give 265 mg (80%).

Synthesis of adipic dihydrazidofunctionalized HA (HA-ADH) HA-ADH was prepared according to the method of Bulpitt and Aeschlimann [36]. Briefly, HA was dissolved in water to give a concentration of 3 mg/ml. To this solution was added a 30-fold molar excess of ADH. The pH of the reaction mixture was adjusted to 6.8 with 0.1 M NaOH/0.1 M HCl. One equivalent of EDCI was added in solid form followed by 1 Eq of 1-hydroxybenzotriazole in dimethyl sulfoxide–H_2O (1:1) solution. The pH of the mixture was maintained at 6.8 by the addition of 0.1 M NaOH, and the reaction was allowed to proceed overnight. The reaction was quenched by the addition of 0.1 N NaOH (pH 7.0). The mixture was then transferred to pretreated dialysis tubing and dialyzed exhaustively against 100 mM NaCl, 25% EtOH/H_2O, and, finally, H_2O. The solution was filtered through a 0.2-μm cellulose acetate membrane, flash frozen, and lyophilized. The purity of HA-ADH was determined by HPLC. The extent of substitution of HA with ADH was determined by the ratio of methylene hydrogens to acetyl methyl protons, as measured by [^{1}H]NMR.

Synthesis of HA-TXL In initial experiments, we followed the method reported by Luo and Prestwich [34] and Luo et al. [35] but were only able to obtain low yields ($\leq$ 10%), which are insufficient to support *in vivo* studies. Instead, we synthesized HA-TXL as described below, with the major change being a higher pH for final coupling, and we were able to consistently obtain moderate to high yields ($\geq$ 50%). HA-ADH (75 mg) was dissolved in 0.1 M $NaHCO_3$ buffer (pH 8.5) at a concentration of 1 mg/ml. To this solution was added Taxol–NHS ester (18 mg) dissolved in sufficient DMF–H_2O (2:1, vol/vol) to give a homogeneous solution. The reaction mixture was stirred at room temperature for 24 hours and then evaporated to dryness *in vacuo* (37°C). The residue was dissolved in H_2O, and the product was purified by gel filtration chromatography (Biogel P-10; Bio-Rad, Hercules, CA) using water as eluent. Fractions containing HA-TXL, as evidenced by HPLC analysis, were combined and lyophilized. The [^{1}H]NMR spectrum of the product showed phenyl resonances at 7.25 to 8.15 ppm, affording proof of HA-TXL formation. The purity of the product was determined by HPLC analysis. The percentage of incorporated paclitaxel was determined by UV absorbance (Taxol: λ_{max} = 227 nm, $\varepsilon = 2.8 \times 10^4$). In this manner, conjugates with up to $\sim$ 10% of the carboxyl groups modified were prepared; this level of substitution would leave $\geq$ 90% of disaccharides intact and available for CD44 binding

and would produce conjugates containing ~ 15% to 20% paclitaxel (wt/wt). For *in vitro* and *in vivo* studies, paclitaxel equivalents in terms of concentration and mass, respectively, were calculated for each batch of prepared HA-TXL.

In Vitro *Cytotoxicity Assays*

NMP-1 and SKOV-3ip cells (1×10^4 cells/well) were cultured overnight in 96-well plates in 100 μl of medium (Dulbecco's modified Eagle's medium/F12; Life Technologies, Inc., Gaithersburg, MD) supplemented with 5% fetal calf serum/well before treatment. The cytotoxic effects of HA-TXL were established using a dose range of up to 4 μg/ml (paclitaxel equivalents). Remaining viable cells were stained with neutral red after up to 96 hours, and the percentage of control cell survival as measured by the optical density of incorporated dye was determined. The results from two to four experiments of each type are shown. In competition studies, cells were pretreated with a 100-fold molar excess of free HA before 4 hours of incubation with HA-TXL; free HA and HA-TXL were washed off the plate, and fresh medium was added for the rest of the 72-hour incubation period.

In Vivo *Efficacy Assays*

NMP-1 This study was designed to give quantitative survival data as criteria for the antitumor efficacy of HA-TXL and for its comparison to Taxol. On day 0, about 1×10^7 viable NMP-1 cells were injected into the peritoneal cavities of groups of 6- to 9-week-old female nude mice (Harlan Sprague Dawley, Indianapolis, IN). Five or more mice per experimental group were used as the basis for statistical analyses. Administration of drugs was initiated 1 week later (day 7). Complete necropsy and histopathological evaluation, as well as MR imaging analysis, of mice in parallel studies indicated that, within 7 days of intraperitoneal inoculation, abdominal tumors were already present [15,37]. Taxol was administered intraperitoneally on a schedule of every 7 days × 3, at either 10 or 15 mg/kg; doses higher than this frequently resulted in marked toxicity and/or death in our hands [15]. HA-TXL (14% paclitaxel by weight) was administered in a single intraperitoneal dose of up to 300 mg/kg in pilot studies, and 180 mg/kg HA-TXL (18% paclitaxel by weight) was used in the main study—the same dose as previously used in preclinical ovarian carcinoma xenograft studies with PGA-TXL [15]. NMP-1–implanted mice developed marked ascites as one of the earliest clinical signs of peritoneal tumor and before other aspects of tumor progression became apparent; ascitic fluid was repeatedly removed from mice at intervals, beginning around the fourth week. Eventually, cachexia, spine prominence, and other morbid symptoms became more severe, and these animals were humanely sacrificed by carbon dioxide asphyxiation. For any tumor-bearing mice that succumbed between daily observations and before the opportunity to sacrifice them, the day of death was considered to be the day before the date they were discovered as deceased. The day of humane sacrifice or death was recorded for each mouse, and these values were compared among control and treatment groups by paired or unpaired Student's *t* test for survival analyses.

SKOV-3ip This study was conducted similarly to those described for the NMP-1 model, except that the mice were subjected to magnetic resonance (MR) imaging–based quantification of remaining tumor volumes at a common end point, rather than being taken to a survival end point. Furthermore, 1×10^6 to 2×10^6 cells were injected intraperitoneally, and treatment with HA-TXL was not initiated until day 14.

MR Imaging Analyses

MR imaging studies were conducted at the M. D. Anderson Cancer Center Small Animal Imaging Facility (SAIF). Previous studies [37] revealed that these orthotopic intraperitoneal human ovarian carcinoma xenograft models initially presented either as numerous widely dispersed foci of individual and coalescing solid tumors throughout the peritoneal cavity or as more solid masses that appeared to originate adjacent to and around the pancreas. Respiratory-gated T_2-weighted (T_E = 45.0 milliseconds; T_R = 1215.6 milliseconds; thickness = 0.5 mm; space between images = 0.3 mm) coronal images were used for the initial evaluation of tumor distribution and growth in these models; images of the abdomens of these mice were acquired using a Bruker 4.7-T, 40-cm *Biospec* MR scanner (Bruker Biospin USA, Billerica, MA). Preliminary studies had demonstrated that peritoneal tumors as small as 500 μm in diameter were detectable; generally, MR imaging–based evidence of tumor was first clearly detected on day 7 (NMP-1) and day 14 (SKOV-3).

In NMP-1 studies, mice were held for survival end points. In SKOV-3ip studies, tumor measurements were performed using the Image J program (National Institutes of Health, Bethesda, MD). Regions of interest were drawn on each image that contained a tumor and then multiplied by slice thickness to obtain tumor volume. If the tumor was seen in several contiguous slices, then tumor volumes were added together. To avoid overestimation of tumor size, one half of the volume from the most dorsal and ventral images containing the tumor was used in volume analysis. Assuming a tumor density of 1 g/ml, tumor volumes (mm^3) were converted to weight (g) for analysis [38].

Results and Discussion

Cytotoxic Specificity of HA-TXL In Vitro

The human ovarian carcinoma cell lines NMP-1 and SKOV-3ip were determined to be CD44(+) by flow cytometry (data not shown). Initial *in vitro* experiments were designed to establish whether the uptake and subsequent cytotoxic effects of HA-TXL on these cell lines were CD44-specific. The results in Table 1 demonstrate that, for both cell lines, preblocking of HA binding sites with free HA inhibited the ability of HA-TXL to reduce target cell survival. This result reflects the predominant role of receptor (CD44)–specific uptake, compared to nonspecific pinocytosis, of HA-TXL; however, the latter route of uptake should still be operant, leading to some non–HA-inhibitable uptake by and cytotoxicity in CD44(+) cells, as well as with CD44(−) cells.

Table 1. Specificity of HA-TXL Cytotoxicity against CD44(+) Human Ovarian Carcinoma Cell Lines: Blocking by Free HA.

HA-TXL	% Survival (4-Hour HA-TXL Treatment)	
	SKOV-3ip	NMP-1
5000 ng/ml	55.9 ± 7.0*	67.6 ± 4.6
+ Free HA†	104.8 ± 9.6‡	86.5 ± 3.7
500 ng/ml	81.8 ± 14.5	73.0 ± 5.2
+ Free HA	101.9 ± 11.3	96.5 ± 4.1‡
50 ng/ml	74.8 ± 12.3	78.7 ± 4.0
+ Free HA	91.6 ± 8.5‡	79.3 ± 4.5

*Mean ± SEM compared to untreated or HA-treated controls.
†One-hundred–fold molar excess HA equivalents, preincubated for 4 hours prior to HA-TXL addition.
‡$P < .03$ (*t*-test) *versus* HA-TXL without preblocking.

These results are in good agreement with those of Luo et al. [35] who demonstrated CD44-specific uptake and internalization of fluorescently labeled HA and cytotoxicity of HA-TXL against CD44(+) SKOV-3 and other tumor cells, whereas HA-TXL was ineffective against CD44(−) NIH 3T3 target cells. The relatively flat dose response of cytotoxicity *versus* HA-TXL concentration in our studies is reminiscent of the response to free Taxol that we have previously observed with NMP-1 and HEY ovarian carcinoma models [15] and, in that light, makes the observed extent of blockade with free HA more compelling.

Preliminary Toxicity Studies of HA-TXL

Mice were injected intraperitoneally with HA-TXL at doses of up to 300 mg/kg (paclitaxel equivalents), and these mice were held for observation for at least 6 months. The mice were found to tolerate even the highest dose administered, indicating that this formulation was far less toxic than free paclitaxel (Taxol). Furthermore, the 250- and 300-mg/kg doses exceeded the highest dose we had previously used (200 mg/kg) with another paclitaxel prodrug PGA-TXL [15], suggesting that HA-TXL might have an even higher mouse MTD than PGA-TXL. It is also considerably higher than the 100-mg/kg dose recently reported as the MTD for another HA–paclitaxel prodrug formulation, HYTAD1-p20 [39].

Antitumor Efficacy of HA-TXL

We next evaluated both MR imaging–based antitumor effects and effects on survival following HA-TXL treatment in CD44(+) NMP-1 and SKOV-3ip orthotopic (intraperitoneal) xenograft models.

NMP-1 In a pilot efficacy experiment, mice bearing NMP-1 xenografts received an intraperitoneal injection of HA-TXL (100 or 200 mg/kg, paclitaxel equivalents) on day 8 post–tumor implantation. Control mice survived for an average of 34 days, mice treated with 100 mg/kg HA-TXL survived to day 60, and mice treated with 200 mg/kg HA-TXL were sacrificed on day 199 and judged tumor-free by MR imaging (Figure 1; compare with controls in Figure 3*A*).

In an expanded efficacy experiment, groups of NMP-1–implanted mice were treated either with vehicle, with multiple-dose regimens of Taxol (using 10 or 15 mg/kg; higher doses on this schedule are toxic), or with a single injection of HA-TXL. Effects on survival are shown in the Kaplan-Meier survival plot in Figure 2 and are summarized in Table 2. In addition, two of five mice in each group were MR-imaged on day 28 post–tumor inoculation before any mice required sacrifice. NMP-1–implanted mice responded to HA-TXL treatment with a T/C ~ 140 (Figure 2; $P = .004$ by Mantel-Cox) and showed markedly reduced tumor burden (Figure 3*D*) compared to controls (Figure 3*A*). In contrast, multiple-dose regimens of Taxol at either dose level were essentially inactive in this model, both by MR imaging (Figure 3*B* for 10 mg/kg; Figure 3*C* for 15 mg/kg) and survival criteria (Figure 2; T/C ~ 105 for 10 mg/kg and T/C ~ 120 for 15 mg/kg).

Figure 1. *T_2-weighted coronal MR image of the abdomen of an NMP-1–implanted nude mouse (199 days following tumor inoculation) that was treated with a single intraperitoneal injection of 200 mg/kg HA-TXL 8 days post–tumor inoculation. No tumors were observed; compare to day 28 images of NMP-1 control mice in Figure 3A.*

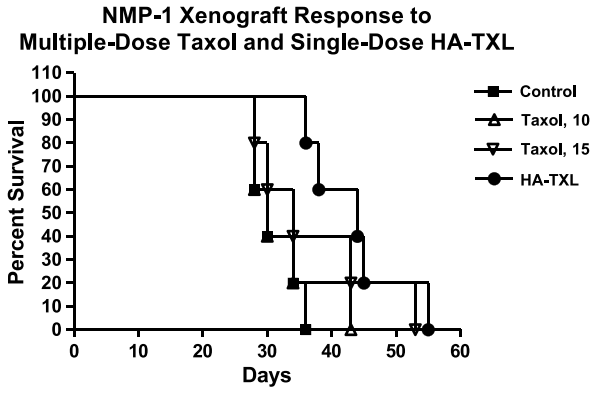

Figure 2. *Kaplan-Meier survival plot of NMP-1–implanted mice treated intraperitoneally either with saline (controls), with 10 or 15 mg/kg Taxol on regimens of every 7 days × 3 beginning on day 7 post–tumor implantation, or with a single injection of 180 mg/kg HA-TXL (paclitaxel equivalents) on day 7. T/C values were 105 and 120 for the 10- and 15-mg/kg multiple-dose Taxol groups, respectively, and 140 for the single-dose HA-TXL group (P = .004 vs controls; Mantel-Cox).*

Table 2. Response of NMP-1 Xenograft Model to Multiple-Dose Taxol and Single-Dose HA-TXL.

Treatment	Mean Day of Survival/Sacrifice	T/C
Control	31.2 ± 3.2*	–
Taxol		
10 mg/kg (every 7 days × 3)†	32.6 ± 5.6	105
15 mg/kg (every 7 days × 3)‡	37.6 ± 9.3	120
HA-TXL, 180 mg/kg§	43.6 ± 6.7	140¶

*Mean ± SEM.
†Taxol regimens initiated on Day 7 post–tumor inoculation.
‡Higher doses caused toxicity on this schedule.
§Single dose administered on Day 7.
¶$P = .004$ *vs* controls (Mantel-Cox).

SKOV-3ip Antitumor efficacy results with HA-TXL were generally similar to those with the SKOV-3ip ovarian carcinoma model. Necropsy examination conducted by a board-certified veterinary pathologist (R.E.P.) on mice from the HA-TXL treatment group found only small tumors 12 weeks post–tumor implantation and 10 weeks posttreatment. However, control SKOV-3ip mice all presented evidence for marked tumor involvement, typically including abdominal distention with bloody ascites and marked abdominal tumor burden associated with the umbilicus, diaphragm, abdominal wall, lymph nodes, and mesentery. MR images obtained on the day of sacrifice were analyzed by a diagnostic imaging clinician (V.K.), and representative images are shown in Figure 4; again, these images show clear distinctions between treated and control groups. Only small tumors were detected in HA-TXL–treated mice (Figure 4*B*), whereas significant tumor burden and resultant abdominal distention were very apparent in control mice (Figure 4*A*). Quantification of contiguous MR images demonstrated that tumor burden in the HA-TXL–treated group was markedly reduced compared to controls ($P < .03$, *t*-test; Figure 4*C*).

Thus, in the SKOV-3ip model, both MR imaging and histopathological analyses support the antitumor efficacy of even a single dose of HA-TXL administered at a sub-MTD level.

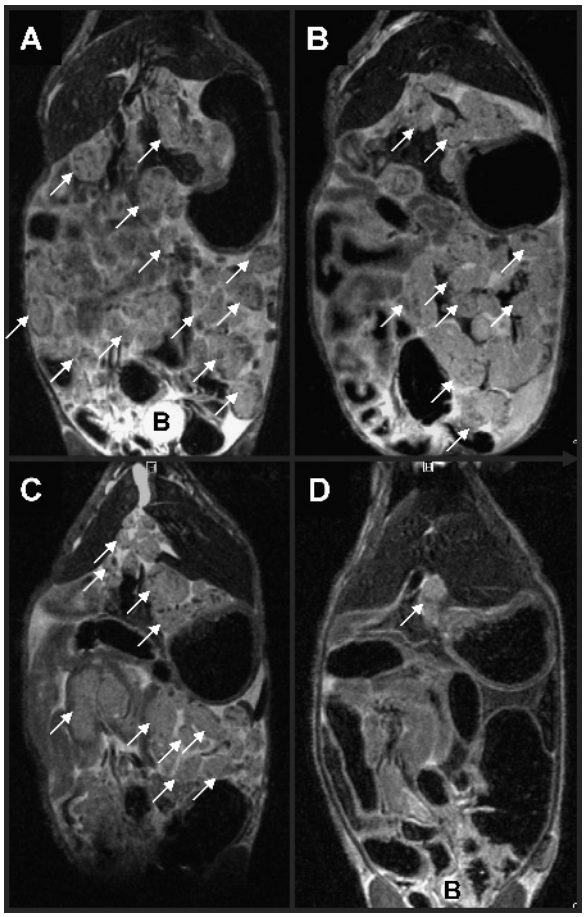

Figure 3. *Representative day 28 T_2-weighted coronal abdominal MR images of NMP-1–implanted (A) control mice sham-treated with saline; arrows indicate examples of tumor masses throughout the abdomen; note the heavy tumor burden and areas of high signal intensity indicating ascites. (B) Mice treated with a multiple-dose intraperitoneal injection regimen of 10 mg/kg Taxol; arrows indicate examples of tumor masses throughout the abdomen; note evidence for ascites. (C) Mice treated with a multiple-dose intraperitoneal injection regimen of 15 mg/kg Taxol; note heavy tumor burden and ascites. (D) Mice treated with a single intraperitoneal injection of HA-TXL; note the comparatively modest tumor burden and few areas of high signal intensity indicating ascites. B = bladder.*

Preliminary Toxicology Studies of HA-TXL

Aside from CD44, which was originally associated with lymphocyte activation, other HA receptors include RHAMM (receptor for HA-mediated cell motility) and HARLEC (HA

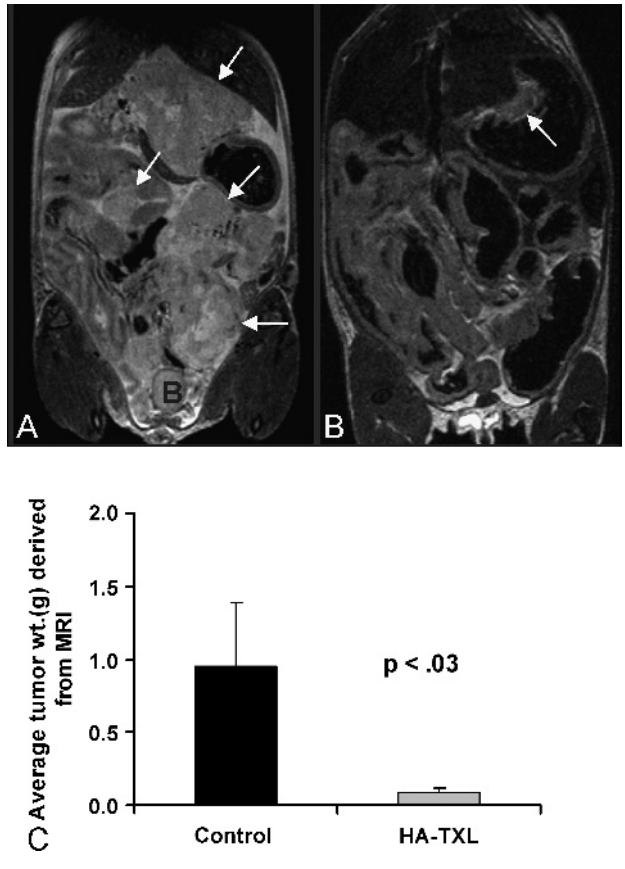

Figure 4. *Representative day 84 coronal T_2-weighted MR images of the abdomens of SKOV-3ip–implanted mice from the control group (A) and the 180-mg/kg HA-TXL treatment group (B). Arrows indicate examples of intraperitoneal tumors; note the greater tumor burden in control versus treated mice. B = bladder. Comparison of tumor weights derived from MR images of mice bearing SKOV-3ip tumors (C; P < .03, n = 3; t-test).*

receptor, liver endothelial cells). Thus, we wanted to determine whether, as a result of the expression of HARLEC or other HA receptors, HA-TXL treatment would be associated with significant hepatotoxicity. In preliminary studies, we observed only a slight elevation of serum liver transaminase (aspartate aminotransferase = 220 U/ml; alanine aminotransferase = 175 U/ml) and alkaline phosphatase (92 U/ml) levels 24 hours after intraperitoneal injection of 180 mg/kg HA-TXL. It is possible that these toxicities were secondary to liver uptake, particularly the transaminase elevations; however, HARLEC and RHAMM are less specific for HA than is CD44, and the former can be blocked with chondroitin sulfate [40]. This preblocking strategy should shunt HA-TXL away from certain normal tissues and increase uptake in tumor.

Our studies focused on CD44(+) human ovarian carcinoma models, and the selectivity of HA-TXL for these CD44-expressing cell lines was demonstrated *in vitro* by competition experiments with free HA (Table 1); similar observations of CD44-specific uptake and cytotoxicity of HA-TXL, as well as lack of effects against CD44(−) NIH 3T3 cells, have been reported previously [34,35]. To further understand the nature of the HA/CD44 interaction and the role it might play in the selectivity of response to HA-TXL *in vivo*, a control study would be of interest using CD44(−) tumor models. However, we have not been able to define a CD44(−) human ovarian carcinoma model, nor another CD44(−) tumor model with peritoneal metastases, for such evaluation. Furthermore, both potentially tumor-promoting and/or tumor-inhibiting effects of free HA in CD44(+) models must be properly controlled for in such analyses. Nevertheless, by employing a similar competition strategy with coadministered free HA, it might be possible to glean the relative roles of receptor-specific *versus* pinocytotic uptake of HA-TXL *in vivo* with CD44(+) tumor models.

Other studies have begun to evaluate the antitumor efficacy of prodrug formulations based on an HA backbone or ligand [37,39,41–43]. For example, butyric acid esters of HA were prepared, and these conjugates were injected intratumorally in a subcutaneously implanted syngeneic Lewis lung carcinoma model. The growth rate of an ectopic tumor was reduced compared to vehicle control, and both the number and the weight of lung metastases were significantly reduced compared to controls [41,42]. Our study differs in several respects, including the use of an orthotopic (intraperitoneal) human tumor xenograft and administration of the HA prodrug locoregionally (intraperitoneal) rather than intratumorally. A recent study is more similar to ours, as it used an HA backbone for a paclitaxel prodrug (HYTAD1-p20) [39]. In an ectopic human bladder carcinoma xenograft model in SCID mice, multiple-dose regimens of HYTAD1-p20 administered intraperitoneally, or Taxol administered intravenously, achieved comparable tumor growth inhibition. Nevertheless, our results in the orthotopic NMP-1 model demonstrate superior antitumor efficacy with even a single dose of HA-TXL compared to a multiple-dose Taxol regimen.

Although we view HA as simply a backbone by which paclitaxel (and other) chemotherapeutics might be delivered to CD44(+) tumor cells, we did not attempt to rule out the possibility that part of the anti-tumor effect of HA-TXL might be mediated by the backbone itself. For example, HA may disrupt CD44(+) tumor cell–extracellular matrix interactions, presumably leading to anoikis, as has been observed in a human breast carcinoma xenograft model [44]. In that light, future comparisons of HA-TXL antitumor efficacy against tumor models with even greater taxane resistance might be informative in distinguishing direct effects on either tumor or stromal compartments.

In view of the recent clinical trial results demonstrating the survival benefit of intraperitoneal *versus* intravenous administration of chemotherapeutic agents for ovarian cancer patients with small-volume peritoneal disease, we confined our preclinical evaluation of HA-TXL to the intraperitoneal administration route. However, this does not exclude the possibility that the intravenous administration route would also demonstrate antitumor efficacy, although such direct exposure to CD44(+) leukocyte populations might have undesired effects on immune function, nor does it address the actual pharmacological behavior and mode of uptake of HA-TXL administered intraperitoneally. Although a reasonable model for the latter would certainly be one involving a direct uptake of HA-TXL from the peritoneum into the tumor milieu, one cannot currently exclude the possibility of clearance from the peritoneum, followed by systemic distribution and extravasation from the tumor vasculature in small tumor foci present at the time of treatment [45]. Furthermore, another setting in which HA-TXL–based therapy might have a sound rationale is in metronomic therapy, as the absence of polyoxyl 40 hydrogenated castor oil (Cremophor; Sigma-Aldrich, St. Louis, MO) would obviate the interference of this excipient with the antiangiogenic effects of taxanes—paclitaxel in particular.

A number of variables to be optimized in future preclinical studies include the size of the HA backbone, as this should affect the rates of HA-TXL clearance from the peritoneum and from the vascular compartment, as well as the opportunity for multiple CD44/HA binding interactions, and hence the resultant avidity. Similarly, the extent of paclitaxel substitution in the current study was intentionally kept at ~ 10% or less of the available carboxyl groups on the HA, with the expectation that this would have a minimal effect on HA/CD44 interactions. However, higher loading may be acceptable, particularly with longer HA chains that allow multiple receptor interactions.

Based on these promising results in antitumor efficacy studies, we conclude that HA-based prodrugs, HA-TXL in particular, merit further preclinical development and evaluation. Furthermore, with increasing evidence for the expression of CD44 on cancer stem cells of diverse origins [46–53], the ability to selectively target chemotherapeutic agents to CD44 may achieve marked significance.

Acknowledgements

We acknowledge James Bankson and the personnel at SAIF for their expertise with MR imaging aspects of this study. We are grateful to Anil Sood for critical reading of this manuscript.

References

[1] Fields MM and Chevlen E (2006). Screening for disease: making evidence-based choices. *Clin J Oncol Nurs* **10** (1), 73–76 (Review).

[2] Morrison J (2005). Advances in the understanding and treatment of ovarian cancer. *J Br Menopause Soc* **11** (2), 66–71 (Review).

[3] Parazzini F, Chiaffarino F, Negri E, Surace M, Benzi G, Franceschi S, Fedele L, and La Vecchia C (2004). Risk factors for different histological types of ovarian cancer. *Int J Gynecol Cancer* **14** (3), 431–436.

[4] Kringen P, Wang Y, Dumeaux V, Nesland JM, Kristensen G, Borresen-Dale AL, and Dorum A (2005). *TP53* mutations in ovarian carcinomas from sporadic cases and carriers of two distinct BRCA1 founder mutations; relation to age at diagnosis and survival. *BMC Cancer* **5**, 134.

[5] Greimel ER, Bjelic-Radisic V, Pfisterer J, Hilpert F, Daghofer F, du Bois A, and Arbeitsgemeinschaft Gynaekologische Onkologie Ovarian Cancer Study Group (2006). Randomized study of the Arbeitsgemeinschaft Gynaekologische Onkologie Ovarian Cancer Study Group comparing quality of life in patients with ovarian cancer treated with cisplatin/paclitaxel *versus* carboplatin/paclitaxel. *J Clin Oncol* **24** (4), 579–586.

[6] Zhao C, Annamalai L, Guo C, Kothandaraman N, Koh SCL, Zhang H, Biswas A, and Choolani M (2007). Circulating haptoglobin is an independent prognostic factor in the sera of patients with epithelial ovarian cancer. *Neoplasia* **9** (1), 1–7.

[7] Ozols RF (2006). Systemic therapy for ovarian cancer: current status and new treatments. *Semin Oncol* **33** (2 Suppl 6), S3–S11 (Review).

[8] Bankhead C (2006). Intraperitoneal therapy for advanced ovarian cancer: will it become standard care? *J Natl Cancer Inst* **98** (8), 510–512.

[9] de Bree E, Rosing H, Michalakis J, Romanos J, Relakis K, Theodoropoulos PA, Beijnen JH, Georgoulias V, and Tsiftsis DD (2006). Intraperitoneal chemotherapy with taxanes for ovarian cancer with peritoneal dissemination. *Eur J Surg Oncol* **32** (6), 666–670.

[10] Armstrong DK, Bundy B, Wenzel L, Huang HQ, Baergen R, Lele S, Copeland LJ, Walker JL, Burger RA, and Gynecologic Oncology Group (2006). Intraperitoneal cisplatin and paclitaxel in ovarian cancer. *N Engl J Med* **354** (1), 34–43.

[11] Li C, Yu DF, Newman RA, Cabral F, Stephens LC, Hunter N, Milas L, and Wallace S (1998). Complete regression of well-established tumors using a novel water-soluble poly(L-glutamic acid)–paclitaxel conjugate. *Cancer Res* **58** (11), 2404–2409.

[12] Li C, Price JE, Milas L, Hunter NR, Ke S, Yu DF, Charnsangavej C, and Wallace S (1999). Antitumor activity of poly(L-glutamic acid)–paclitaxel on syngeneic and xenografted tumors. *Clin Cancer Res* **5** (4), 891–897.

[13] Li C, Newman RA, Wu QP, Ke S, Chen W, Hutto T, Kan Z, Brannan MD, Charnsangavej C, and Wallace S (2000). Biodistribution of paclitaxel and poly(L-glutamic acid)–paclitaxel conjugate in mice with ovarian OCa-1 tumor. *Cancer Chemother Pharmacol* **46** (5), 416–422.

[14] Zou Y, Wu QP, Tansey W, Chow D, Hung MC, Charnsangavej C, Wallace S, and Li C (2001). Effectiveness of water soluble poly(L-glutamic acid)–camptothecin conjugate against resistant human lung cancer xenografted in nude mice. *Int J Oncol* **18** (2), 331–336.

[15] Auzenne E, Donato NJ, Li C, Leroux E, Price RE, Farquhar D, and Klostergaard J (2002). Superior therapeutic profile of poly-L-glutamic acid–paclitaxel copolymer compared with Taxol in xenogeneic compartmental models of human ovarian carcinoma. *Clin Cancer Res* **8** (2), 573–581.

[16] Zou Y, Fu H, Ghosh S, Farquhar D, and Klostergaard J (2004). Antitumor activity of hydrophilic paclitaxel copolymer prodrug using locoregional delivery in human orthotopic non–small cell lung cancer xenograft models. *Clin Cancer Res* **10** (21), 7382–7391.

[17] Phase II clinical trial of XYOTAX in non–small cell lung cancer to continue. *Expert Rev Anticancer Ther* **2** (3), 244–245.

[18] Singer JW, Baker B, De Vries P, Kumar A, Shaffer S, Vawter E, Bolton M, and Garzone P (2003). Poly-(L)-glutamic acid–paclitaxel (CT-2103) [XYOTAX], a biodegradable polymeric drug conjugate: characterization, preclinical pharmacology, and preliminary clinical data. *Adv Exp Med Biol* **519**, 81–99 (Review).

[19] Langer CJ (2004). Dilemmas in management: the controversial role of chemotherapy in PS 2 advanced NSCLC and the potential role of CT-2103 (XYOTAX). *Oncologist* **9** (4), 398–405 (Review).

[20] Boddy AV, Plummer ER, Todd R, Sludden J, Griffin M, Robson L, Cassidy J, Bissett D, Bernareggi A, Verrill MW, et al. (2005). A phase I and pharmacokinetic study of paclitaxel poliglumex (XYOTAX), investigating both 3-weekly and 2-weekly schedules. *Clin Cancer Res* **11** (21), 7834–7840.

[21] Dipetrillo T, Milas L, Evans D, Akerman P, Ng T, Miner T, Cruff D, Chauhan B, Iannitti D, Harrington D, et al. (2006). Paclitaxel poliglumex (PPX-XYOTAX) and concurrent radiation for esophageal and gastric cancer: a phase I study. *Am J Clin Oncol* **29** (4), 376–379.

[22] Albain KS, Belani CP, Bonomi P, O'Byrne KJ, Schiller JH, and Socinski M (2006). PIONEER: a phase III randomized trial of paclitaxel poliglumex *versus* paclitaxel in chemotherapy-naive women with advanced-stage non–small-cell lung cancer and performance status of 2. *Clin Lung Cancer* **7** (6), 417–419.

[23] Gardner MJ, Catterall JB, Jones LM, and Turner GA (1996). Human ovarian tumor cells can bind hyaluronic acid *via* membrane CD44: a possible step in peritoneal metastasis. *Clin Exp Metastasis* **14**, 325.

[24] Stickeler E, Runnebaum IB, Mobus VJ, Kieback DG, and Krienberg R (1997). Expression of CD44 standard and variant isoforms v5, v6 and v7 in human ovarian cancer cell lines. *Anticancer Res* **17**, 1871.

[25] Yeo TK, Nagy JA, Yeo KT, Dvorak HF, and Toole BP (1996). Increased hyaluronan at sites of attachment to mesentery by CD44-positive mouse ovarian and breast tumor cells. *Am J Pathol* **148**, 1733.

[26] Cannistra SA, Kansas GS, Niloff J, DeFranzo B, Kim Y, and Ottensmeier C (1993). Binding of ovarian cancer cells to peritoneal mesothelium *in vitro* is partly mediated by CD44H. *Cancer Res* **53**, 3830.

[27] Cannistra SA, Abu-Jawdeh G, Niloff J, Strobel T, Swanson L, Andersen J, and Ottensmeier C (1995). CD44 variant expression is a common feature of epithelial ovarian cancer: lack of association with standard prognostic factors. *J Clin Oncol* **13**, 1912.

[28] Kayastha S, Freedman AN, Piver MS, Mukkamalla J, Romero-Guittierez M, and Werness BA (1999). Expression of the hyaluronan receptor, CD44S, in epithelial ovarian cancer is an independent predictor of survival. *Clin Cancer Res* **5**, 1073–1076.

[29] Sillanpaa S, Anttila MA, Voutilainen K, Tammi RH, Tammi MI, Saarikoski SV, and Kosma VM (2003). CD44 expression indicates favorable prognosis in epithelial ovarian cancer. *Clin Cancer Res* **9** (14), 5318–5324.

[30] Kalpna M, Zhang L, Klostergaard J, and Donato NJ (2000). Emergence of CDDP-resistant cells from OVCAR-3 ovarian carcinoma cell line with *p53* mutations, altered tumorigenicity and increased apoptotic sensitivity to *p53* gene replacement. *Int J Gynecol Cancer* **10**, 105–114.

[31] Hamilton TC, Young RC, McKoy WM, Grotzinger KR, Green JA, Chu EW, Whang-Peng J, Rogan AM, Green WR, and Ozols RF (1983). Characterization of a human ovarian carcinoma cell line (NIH: OVCAR-3) with androgen and estrogen receptors. *Cancer Res* **43**, 5379–5389.

[32] Dini MM, Jafari K, and Faiferman I (1980). Cell-mediated cytotoxicity in preinvasive and invasive squamous cell carcinoma of the cervix. *Obstet Gynecol* **55**, 728–731.

[33] Buick RN, Pullano R, and Trent JM (1985). Comparative properties of five human ovarian adenocarcinoma cell lines. *Cancer Res* **45**, 3668–3676.

[34] Luo Y and Prestwich GD (1999). Synthesis and selective cytotoxicity of a hyaluronic acid–antitumor bioconjugate. *Bioconjug Chem* **10** (5), 755–763.

[35] Luo Y, Ziebell MR, and Prestwich GD (2000). A hyaluronic acid–Taxol antitumor bioconjugate targeted to cancer cells. *Biomacromolecules* **1** (2), 208–218.

[36] Bulpitt P and Aeschlimann D (1999). New strategy for chemical modification of hyaluronic acid: preparation of functionalized derivatives and their use in the formation of novel biocompatible hydrogels. *J Biomed Mater Res* **47**, 152–169.

[37] Klostergaard J, Auzenne E, Ghosh S, Farquhar D, Rivera B, and Price RE (2006). Magnetic resonance imaging-based prospective detection of intraperitoneal human ovarian carcinoma xenografts treatment response. *Int J Gynecol Cancer* **16** (Suppl 1), 111–117.

[38] Yang D, Han L, and Kundra V (2005). Exogenous gene expression in tumors: noninvasive quantification with functional and anatomic imaging in a mouse model. *Radiology* **235** (3), 950–958.

[39] Rosato A, Banzato A, De Luca G, Renier D, Bettella F, Pagano C, Esposito G, Zanovello P, and Bassi P (2006). HYTAD1-p20: a new paclitaxel–hyaluronic acid hydrosoluble bioconjugate for treatment of superficial bladder cancer. *Urol Oncol* **24**, 207–215.

[40] Mahteme H, Graf W, Larsson BS, and Gustafson S (1998). Uptake of hyaluronan in hepatic metastases after blocking of liver endothelial cell receptors. *Glycoconj J* **15** (9), 935–939.

[41] Coradini D, Pellizzaro C, Abolafio G, Bosco M, Scarlata I, Cantoni S, Stucchi L, Zorzet S, Turrin C, Sava G, et al. (2004). Hyaluronic-acid butyric esters as promising antineoplastic agents in human lung carcinoma: a preclinical study. *Invest New Drugs* **22** (3), 207–217.

[42] Speranza A, Pellizzaro C, and Coradini D (2005). Hyaluronic acid butyric esters in cancer therapy. *Anticancer Drugs* **16** (4), 373–379 (Review).

[43] Peer D and Margalit R (2004). Tumor-targeted hyaluronan nanoliposomes increase the antitumor activity of liposomal doxorubicin in syngeneic and human xenograft mouse tumor models. *Neoplasia* **6** (4), 343–353.

[44] Herrera-Gayol A and Jothy S (2002). Effect of hyaluronan on xenotransplanted breast cancer. *Exp Mol Pathol* **72**, 179–185.

[45] El-Kareh AW and Secomb TW (2004). A theoretical model for intraperitoneal delivery of cisplatin and the effect of hyperthermia on drug penetration distance. *Neoplasia* **6** (2), 117–127.

[46] Walton JD, Kattan DR, Thomas SK, Spengler BA, Guo HF, Biedler JL, Cheung NK, and Ross RA (2004). Characteristics of stem cells from human neuroblastoma cell lines and in tumors. *Neoplasia* **6** (6), 838–845.

[47] Gibbs CP, Kukekov VG, Reith JD, Tchigrinova O, Suslov ON, Scott EW, Ghivizzani SC, Ignatova TN, and Steindler DA (2005). Stem-like cells in bone sarcomas: implications for tumorigenesis. *Neoplasia* **7** (11), 967–976.

[48] Jin L, Hope KJ, Zhai Q, Smadja-Joffe F, and Dick JE (2006). Targeting of CD44 eradicates human acute myeloid leukemic stem cells. *Nat Med* **12** (10), 1167–1174.

[49] Phillips TM, McBride WH, and Pajonk F (2006). The response of CD24(−/low)/CD44$^+$ breast cancer–initiating cells to radiation. *J Natl Cancer Inst* **98** (24), 1777–1785.

[50] Ponti D, Zaffaroni N, Capelli C, and Daidone MG (2006). Breast cancer stem cells: an overview. *Eur J Cancer* **42** (9), 1219–1224 (Review).

[51] Li C, Heidt DG, Dalerba P, Burant CF, Zhang L, Adsay V, Wicha M, Clarke MF, and Simeone DM (2007). Identification of pancreatic cancer stem cells. *Cancer Res* **67** (3), 1030–1037.

[52] Prince ME, Sivanandan R, Kaczorowski A, Wolf GT, Kaplan MJ, Dalerba P, Weissman IL, Clarke MF, and Ailles LE (2007). Identification of a subpopulation of cells with cancer stem cell properties in head and neck squamous cell carcinoma. *Proc Natl Acad Sci USA* **104** (3), 973–978.

[53] Tang DG, Patrawala L, Calhoun T, Bhatia B, Choy G, Schneider-Broussard R, and Jeter C (2007). Prostate cancer stem/progenitor cells: identification, characterization, and implications. *Mol Carcinog* **46** (1), 1–14 (Review).